

RESEARCH

Open Access



DoSPX1 and DoMYB37 regulate the expression of *DoCSLA6* in *Dendrobium officinale* during phosphorus starvation

ZhiYuan Feng^{1†}, YaWen Li^{1†}, SiXue Zhang¹, Jingjing Song¹, HaoXin Xiang¹, JunRu Huang¹, HongHong Fan^{1,2*} and Lin Liu^{1*}

Abstract

Background *Dendrobium officinale* Kimura et Migo (*D. officinale*) is parasitic on rocks or plants with very few mineral elements that can be absorbed directly, so its growth and development are affected by nutritional deficiencies. Previous studies found that phosphorus deficiency promotes polysaccharides accumulation in *D. officinale*, the expression of *DoCSLA6* (glucomannan synthase gene) was positively correlated with polysaccharide synthesis. However, the molecular mechanism by which the low phosphorus environment affects polysaccharide accumulation remains unclear.

Results We found that DoSPX1 can reduce phosphate accumulation in plants and promote the expression of *PSIs* genes, thereby enhancing plant tolerance to low phosphorus environments. Y1H and EMSA experimental show that DoMYB37 can bind the promoter of *DoCSLA6*. DoSPX1 interact with DoMYB37 transiently overexpressed *DoSPX1* and *DoMYB37* in *D. officinale* protocorm-like bodies, decreased the Pi content, while increased the expression of *DoCSLA6*.

Conclusions The signaling pathway of DoSPX1-DoMYB37-*DoCSLA6* was revealed. This provides a theoretical basis for the accumulation of polysaccharide content in *D. officinale* under phosphorus starvation.

Keywords *Dendrobium officinale*, Phosphorus starvation, MYB family, Glucomannan

Background

D. officinale which is the second largest genus in the orchid family is a perennial epiphytic herb. *D. officinale* has a variety of pharmacological effects including

antioxidant and immune-enhancing properties [1–3]. Mannose and glucose were the most abundant monosaccharide component in soluble polysaccharides, and were the most important component affecting the efficacy of soluble polysaccharides [4, 5]. The total polysaccharide and mannose content are quantitative indicators of *D. officinale* [6].

Phosphorus (Pi) plays an important role in various physiological processes in plants. The majority of the phosphorus in the soil forms adsorbed states, resulting in long-term phosphorus deficiency in plants [7–9]. *D. officinale* is generally attached to large tree trunks in primitive forests, shady and damp cliffs, and rock crevices. It is important to study how *D. officinale* ironwood absorbs and utilizes phosphate and accumulates polysaccharides

[†]ZhiYuan Feng and YaWen Li contributed equally to this work.

*Correspondence:

HongHong Fan
hhfan0551@126.com

Lin Liu
liulin2018@ahau.edu.cn

¹ School of Life Sciences, Anhui Agricultural University, Hefei, Anhui 230036, People's Republic of China

² Integrated Experimental Station in Dabie Mountains, Anhui Agricultural University, Lu'an, China



in this growth environment. Our previous study founded that inorganic phosphate (Pi) deficiency promoted the accumulation of *D. officinale* polysaccharides [10]. Under LP environments, the expression of *DoCSLA6*, a member of the *CSLA* family directly involved in mannose synthesis, was highly positively correlated with the polysaccharide accumulation [10, 11]. However, the molecular mechanism of polysaccharide accumulation induced by low phosphorus in *D. officinale* remains unclear.

The SPX domain was coined based on the first three letters of Suppressor of Yeast *gpa1* (SYG1), Phosphatase 81 (PHO81) and Xenotropic and Polytopic Retrovirus receptor1 (XPR1). Proteins with the SPX domain have been identified as the most important regulators of plant responses to LP, SPX usually works with downstream transcription factors [12–15]. In soybean, GmSPX1 is a negative regulator in response to phosphorus signaling. GmMYB48 is a phosphate starvation-inducible transcription factor. *GmSPX1* overexpression decreased the transcripts of *AtMYB4*, an ortholog of GmMYB48. [16]. In *Arabidopsis thaliana*, AtSPX4 can interact with AtPAP1 to regulate anthocyanin synthesis in a phosphate-dependent manner [17]. Phylogenetic analysis suggests that DoSPX1 may be involved in LP signaling pathway in *D. officinale* [18].

In this study, we analyze the function of DoSPX1 and DoMYB37 by overexpression of DoSPX1 and DoMYB37 in *Nicotiana tabacum* L. (*N. tabacum*) and *D. officinale* protocorm-like bodies. We confirmed the interaction between *DoSPX1* and *DoMYB37* by Yeast Two-Hybrid Assay (Y2H) and Bimolecular fluorescence complementation (BiFC). We also verified the transcriptional regulation of *DoCSLA6* by DoMYB37.

Materials and methods

Plant materials and growth conditions

D. officinale were selected from the Engineering Technology Research Center for the Development and Utilization of Local Characteristic Plant Resources in Anhui Province, Anhui Agricultural University. The *D. officinale* was cultured in MS medium with a light period of 16 h and incubation temperature of 25 degrees Celsius.

Nicotiana tabacum and *Yunyan* seedlings were cultured on Murashige and Skoog (MS) medium at 25 °C, which were lighted for 16 h and dark for 8 h.

Plants were cultured under phosphorus concentrations of 0.0625 mM (LP) and 1.25 mM (NP) master mixes (Supplementary Table 1). MS media with different phosphorus concentrations were prepared using the same molar concentration of KCl instead of KH_2PO_4 .

Quantitative real-time PCR (qRT-PCR)

The RNA was extracted from the Liquid nitrogen quick-frozen plant tissues using the Plant Total RNA Isolation Kit. A One Step RT-qPCR Kit was used to obtain cDNA. $2\times$ TaqMan Fast qPCR Master Mix was used to execute qRT-PCR. Reaction conditions were performed according to Liu's method [10]. The qRT-PCR primers were designed using NCBI PRIMER-BLAST8 (Supplementary Table 2). The relative quantitative analysis method ($2^{-\Delta\Delta\text{CT}}$) was used to calculate the relative gene expression, and all experiments were repeated with more than three biological replicates.

Subcellular localization analysis

To analyze the subcellular localization of the DoSPX1 and DoMYB37 protein, the open reading frame (ORF) was amplified by PCR from the *D. officinale* cDNA library with *DoSPX1* (LOC110102021) and *DoMYB37* (LOC110099272) gene-specific primers (Supplementary Table 2) and inserted into the plant expression vector pCAMBIA1305.1-GFP to generate the pCAMBIA1305.1-DoSPX1 and pCAMBIA1305.1-DoMYB37 construct. Cells of the GV3101-pSoup-p19 carrying pCAMBIA1305.1-DoSPX1/DoMYB37 and pCAMBIA1305.1-GFP (positive control) were separately infiltrated into *Nicotiana tabacum*. Transient expression of GFP signals were observed using a laser confocal microscope after 2 d of infiltration.

Yeast two hybrid (Y2H)

The full-length ORF of *DoSPX1* and *DoMYB37* were constructed on pGADT7 and pGBKT7 respectively. Recombinant vector pGADT7-DoSPX1 and pGBKT7-DoMYB37 were expressed in AH109 strains. Then transformed clones were screened on SD-WL (SD medium without Leu and Trp), and clones were screened on SD-HAWL (SD medium without Ade, His, Leu, and Trp). X- α -Gal is used to identify positive interactions.

Bimolecular fluorescent complementary assay (BiFC)

The full-length ORF of *DoSPX1* and *DoMYB37* were constructed on pCAMBIA2300s-YC and pCAMBIA1300s-YN respectively. Single colonies of *Agrobacterium* were picked and propagated in YEP medium and incubated in a shaker at 28 °C for 24 h. The bacterial sap was collected by centrifugation and resuspended to $\text{OD}_{600}=0.2$ using onion infestation solution, fresh red onions were taken, the epidermis was removed from the third or inner scale, immersed in the onion infestation solution, and incubated in the dark for 30 min. After the infestation, the excess was aspirated from the epidermis using filter paper and incubated for 20–24 h at 22 °C in the dark, and

the fluorescence signal was observed using a laser confocal microscope.

Yeast one-hybrid assay (Y1H)

The *DoCSLA6* promoter cis-acting elements were predicted using the online tools PlantCARE (<http://bioinformatics.psb.ugent.be/webtools/plantcare/html/>) and New PLACE (<https://www.dna.affrc.go.jp/PLACE/?action=newplace>) [19].

The gene promoter is expressed at the background level in *Saccharomyces cerevisiae* Y1Hgold and the minimum/critical ABA concentration for growth inhibition is determined by adding different concentrations of ABA to inhibit the interaction of the promoter fragment itself. The complete *DoMYB37* ORF sequence was constructed on the pGADT7 vector to form a recombinant vector, and the MBS in the promoters of *DoCSLA6* of glucomannan biosynthesis were constructed on the pABAI vector. The *DoMYB37* recombinant plasmids were expanded and cultured with the pGADT7 vector attached and the plasmids were extracted for use. The yeast strain containing the target promoter was prepared as receptor cells and the transformed strain was coated onto SD/-Leu plates with appropriate concentrations of ABA and incubated at 28 °C for 2–3 d. Then the positive colony was picked and tested for growth of monoclonal strains on SD/-Leu medium for 48 h. Empty vectors pGADT7 were used as negative controls.

Electrophoretic mobility shift assay (EMSA)

The target gene promoter sequences were analyzed through the NEWPLACE online (<https://www.dna.affrc.go.jp/PLACE/?action=newplace>) and the promoter probes were designed. The ORF of *DoMYB37* was inserted into the vector pGEX4T-1. Recombinant protein *DoMYB37*-GST was expressed in *E. coli* BL21 (DE3) and purified using a protein purification kit with a GST-tag. Probes were mixed in equal proportions upstream and downstream, denatured at 100 °C for 10 min, and then slowly brought to room temperature and set aside. *DoMYB37*-GST purified protein was combined with probes of pro*DoCSLA6* by adding 5×binding buffer at 25 °C for 25 min. Then 6×Loading Buffer was added to the system and the sample was loaded and electrophoresed at 120 V for 45 min. After electrophoresis, the PAGE gel was removed and stained with nucleic acid dye for 15 min and the results were observed using a gel imager (Shanghai Tanon).

N. tabacum conversion methods

To analyze the *DoSPX1* and *DoMYB37*, The ORF of *DoSPX1* and *DoMYB37* was inserted into the pCAMBIA1305.1 vector. *Agrobacterium tumefaciens* was

expanded and collected and resuspended in infestation solution to $OD_{600}=0.4-0.6$ and set aside. *N. tabacum* with 2–4 true leaves were cut out and placed in dark culture in MS budding medium for 3 days. The dark-cultured leaves were placed in the infestation solution, blotted on filter paper to dry the surface of the infestation solution, and raised in solid medium containing acetosyringone for 3 d. The leaves were washed 2–3 times with sterile water containing Temetin, blotted on filter paper to dry the surface liquid, placed in MS germination medium and incubated at 28 °C in the light, and decolonized again within two weeks. *N. tabacum* shoots up to 1 cm in length were placed in MS empty medium for rooting, and after rooting, the seedlings were transplanted.

Transformation of *D. officinale* protocorm-like bodies

In this laboratory, seeds were used as explants to induce *D. officinale* protocorm-like bodies, and the experimental materials were preserved by the laboratory, and their traits were genetically stable. *D. officinale* protocorm-like bodies were incubated in the dark for 3 days and the *Agrobacterium* introduced into the plasmid was expanded and cultured. Bacteria were collected and resuspended in an infestation solution to $OD_{600}=0.4-0.6$. After washing 2–3 times in sterile water containing antibiotics, the surface was dried with filter paper and then placed in a decontamination medium for sterilization and screening (Supplementary Fig. 1).

Determine the Soluble phosphorus content of plants

Determination of soluble Pi content of plant materials by ammonium molybdate method. We grind the plants with liquid nitrogen and 10% sodium perchlorate, then dilute the supernatant tenfold with 5% (w/v) perchloric acid, centrifuge, and then tenfold with 5% (w/v) perchloric acid. Working solution [ammonium sulfate-molybdate (solution A) and ascorbic acid (solution B) mixed in a ratio of (6:1)]. Calculate the phosphorus content by measuring the absorbance at 820 nm using a UV spectrophotometer.

Results

Overexpression of *DoSPX1* in *N. tabacum*

We first verified the subcellular localization of *DoSPX1*, the ORF of *DoSPX1* was inserted into the pCAMBIA1305.1 vector. The results showed that the fusion protein *DoSPX1*-GFP was mainly distributed in the nucleus (Supplementary Fig. 2). At the same time, we constructed tobacco overexpression lines of *DoSPX1*. Compared to *N. tabacum* transferred with pCAMBIA1305 empty vector, *DoSPX1* transgenic *N. tabacum* showed a significant reduction in leaf number and a significant increase in root length and Root to Shoot ratio, 1.34 and 3.82 times

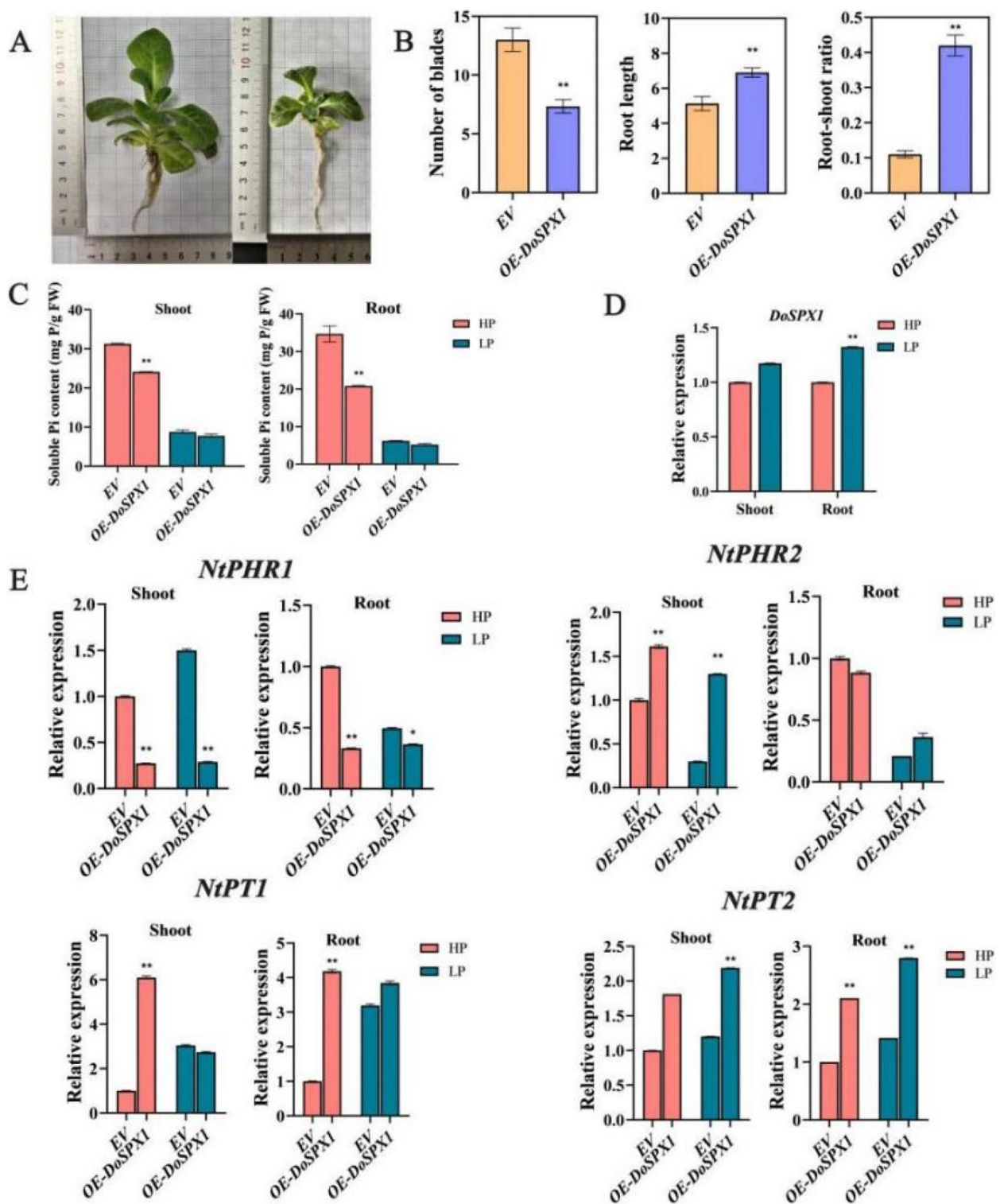


Fig. 1 Phenotype and gene expression in *OE-DoSPX1* transgenic *N. tabacum* and empty vector (control group). **A** *OE-DoSPX1* transgenic *N. tabacum* (The right) and control group (The left). **B** Phenotypic (number of blades, root length, root-shoot ratio) differences in *OE-DoSPX1* *N. tabacum* and control group. **C** Soluble phosphorus content in *OE-DoSPX1* *N. tabacum* and control group. **D** Expression of *DoSPX1* in *OE-DoSPX1* *N. tabacum* and control group. **E** Expression of *PSI* genes (*NtPHR1*, *NtPHR2*, *NtPT1*, *NtPT2*) in *OE-DoSPX1* *N. tabacum* and control group. Significant differences between the Empty vector and *OE-DoSPX1* seedlings grown under the same conditions (HP and LP) are indicated using asterisks (** $p < 0.01$; * $p < 0.05$; two-tailed Student's t-test)

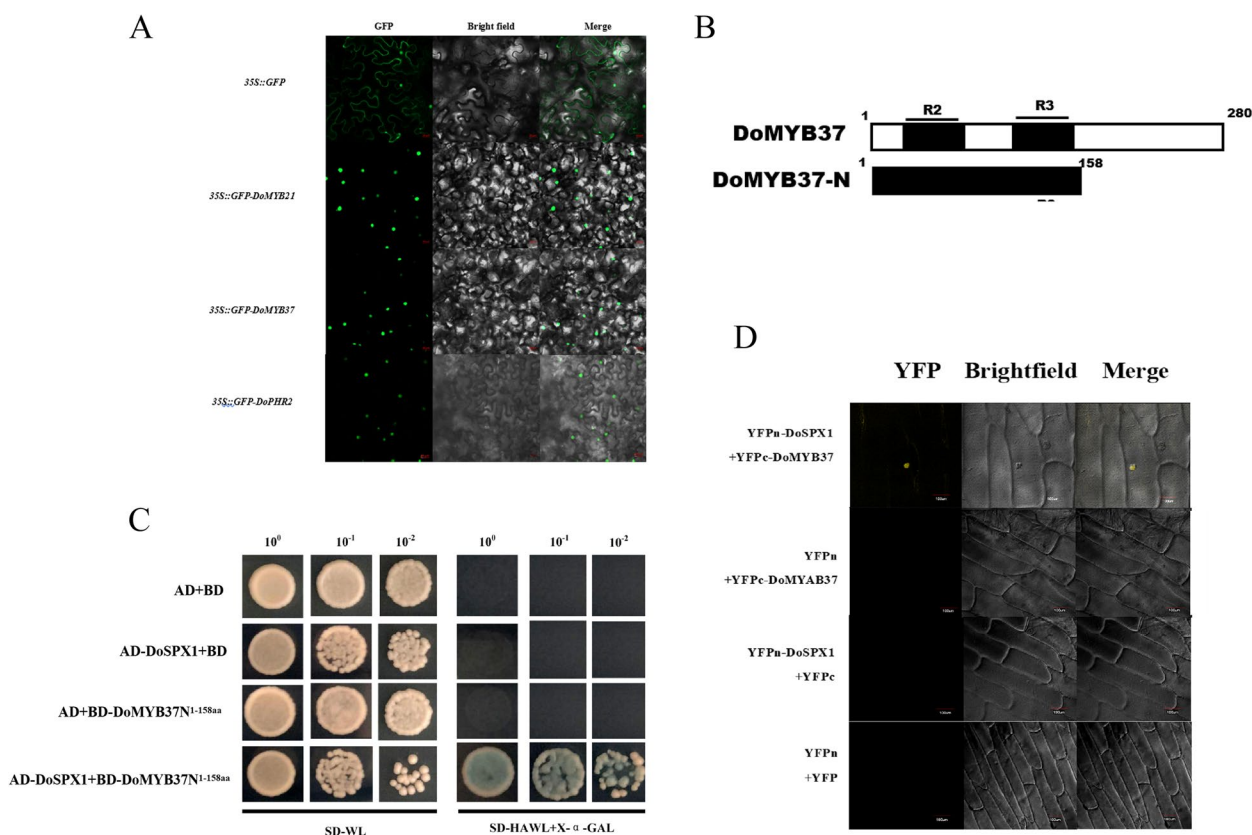


Fig. 2 Subcellular localization of DoMYB37 and interaction between DoMYB37 and DoSPX1. **A** Subcellular localization of DoMYB37. **B** Structural domain analysis and truncation of DoMYB37 proteins. **C** Yeast two-hybridization of DoMYB37-N with DoSPX1. **D** BiFC analysis (YFP: Yellow fluorescent signals)

higher than the control, respectively (Fig. 1A, B). The Pi content of stems and roots in transgenic *N. tabacum* decreased under low phosphorus treatment compared to the control (Fig. 1C). The relative expression of *DoSPX1* was significantly increased by phosphorus starvation, and the changes were more pronounced in the roots (Fig. 1D). When plants are stressed by LP, a large number of Pi starvation-induced (*PSI*) genes, such as phosphorus starvation response (PHRs), phosphate transporters (PTs) are induced. In the *OE-DoSPX1* transgenic lines, *PSI* genes were promoted more obviously by LP (Fig. 1E). These studies suggest that *DoSPX1* overexpression can reduce phosphate accumulation in plants and promote the expression of *PSI*s genes, thereby enhancing plant tolerance to LP environments.

DoMYB37 responds to LP environment and interacts with DoSPX1

Many other researchers have previously found that the 20th subfamily R2R3-MYB are response to phosphate deficiency. Phylogenetic evolutionary showed that DoMYB37 belongs to the 20th subfamily of the MYB

family. The expression levels of *DoMYB37* were increased with decreasing phosphorus concentration in *D. officinale* (Supplementary Fig. 3).

DoMYB37-GFP are subcellular localized to the nuclear (Fig. 2A). To identify the interaction between DoMYB37 and DoSPX1, we divide DoMYB37 into N and C terminals. (Fig. 2B). The Y2H showed that DoMYB37-N grew with the yeast strain of DoSPX1 and showed blue color, indicated that DoSPX1 interacted with the N-terminal of DoMYB37 (Fig. 2C). BiFC verified the interaction of DoMYB37 and DoSPX1 in onion cells, and the YFP signaling is localized in the nucleus of onion cells (Fig. 2D).

Functional identification of DoMYB37 in *N. tabacum* and *D. officinale*

Transgenic *N. tabacum*. overexpressing *DoMYB37* had shorter stems and longer root systems compared with the control group (Fig. 3A). *OE-DoMYB37 N. tabacum* plants had 1.27 times longer root length compared to the empty vector (Fig. 3B). The expression levels of *NtPT1/2* were significantly elevated in *OE-DoMYB37 N. tabacum*

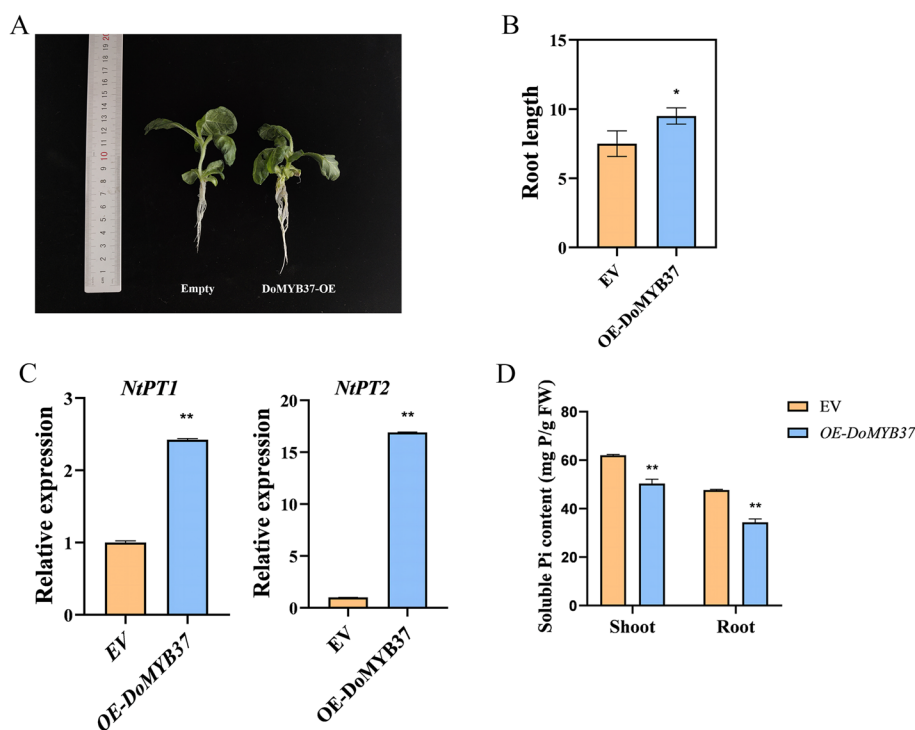


Fig. 3 Root length and related gene expression in *OE-DoMYB37* transgenic *N. tabacum* and empty vector. **A** *OE-DoMYB37* transgenic *N. tabacum*. **B** Root length of *OE-DoMYB37* transgenic *N. tabacum* and empty vector. **C** Expression levels of *NiPT1* and *NiPT2* in *OE-DoMYB37* transgenic *N. tabacum* and empty vector. **D** Soluble phosphorus content in *OE-DoMYB37* transgenic *N. tabacum* and empty vector. Significant differences between the Empty vector and *OE-DoMYB37* seedlings grown under the same conditions (HP and LP) are indicated using asterisks (** $p < 0.01$; * $p < 0.05$; two-tailed Student's t-test)

(Fig. 3C). The soluble phosphorus content in the above-ground part of the *OE-DoMYB37* group was reduced by 0.72-fold, while the soluble phosphorus content in the below-ground part was reduced by 0.81-fold compared to the empty vector (Fig. 3D). This indicates that overexpression of *DoMYB37* reduces phosphate content, which promotes the expression of phosphate transporter proteins *NiPT1*/*NiPT2* and changes in root conformation.

In order to study the function of *DoMYB37*, we established a transient transformation system for the *D. officinale* protocorm-like bodies (Fig. 4A). We obtained the *OE-DoMYB37 D. officinale* protocorm-like bodies, LP promoted the expression level of *DoMYB37* in the control and overexpression groups (Fig. 4B). Soluble phosphorus content in *OE-DoMYB37* was reduced (Fig. 4C). The expression levels of the acid phosphatase genes (*DoPAP17*, *DoPAP2*) and *DoPHT2* became higher in *OE-DoMYB37* transgenic *D. officinale* protocorm-like bodies and were induced by LP (Fig. 4D). In addition, we found that genes related to glucomannan metabolism (*DoGMP*, *DoPMM*, and *DoCSLA6*) expressed at higher levels in overexpressing line than in the control group, and the expression levels of these genes were higher in the LP treatment compared to the HP (Fig. 4D). *D. officinale*

protocorm-like bodies with transiently transformed *DoMYB37* had lower phosphorus content than the control group. The above results showed that overexpression of *DoMYB37* decreased the phosphorus content. Then the expression levels of the *DoPAP17*, *DoPAP2* and *DoPHT2* were increased, which was similar to the results of overexpression of *DoSPX1*.

DoMYB37 binds to the DoCSLA6 promoter and regulates DoCSLA6 expression

DoCSLA6 may be involved in LP-induced mannose accumulation [10]. In addition, *DoCSLA6* expression was significantly higher in *D. officinale* protocorm-like bodies overexpressing *DoMYB37*. Analysis of *DoCSLA6* promoter sequence revealed a large number of MYB binding sites. Three fragments containing MBS elements (a binding site for the MYB transcription factor) in the *DoCSLA6* promoter region (Fig. 5A). Yeast one-hybrid (Y1H) assays showed that *DoMYB37* could bind the three MBS sites on the *DoCSLA6* promoter. (Fig. 5B). The results of EMSA experiments showed that *DoMYB37* can combine with the promoter regions of the *DoCSLA6* (Fig. 5C). We transiently co-transformed *DoSPX1* and *DoMYB37* into protocorm-like bodies and found that

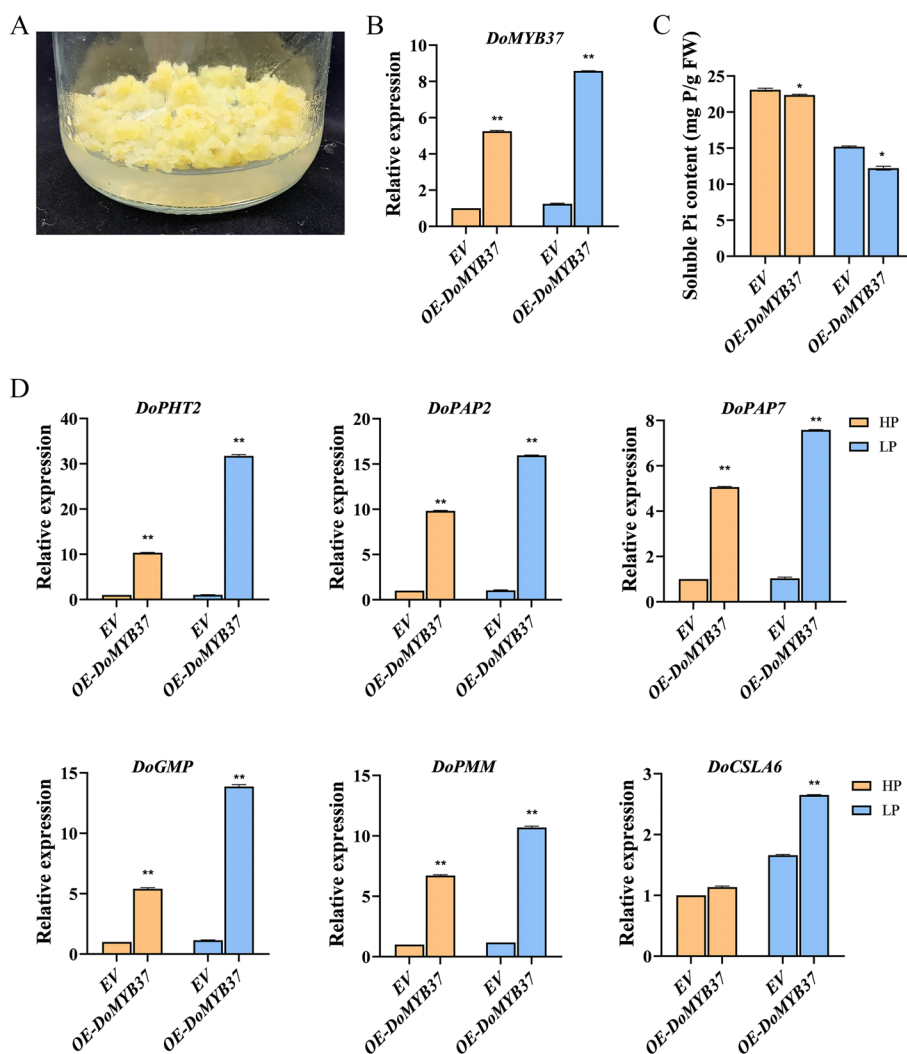


Fig. 4 Physiological indices in OE-DoMYB37 *D. officinale* protocorm-like bodies and control group. **A** *D. officinale* protocorm-like bodies, **B** Expression levels of *DoMYB37*, **C** Soluble phosphorus content, **D** Expression levels of *PSI* genes (*DoPHT2*, *DoPAP2*) and related to gluconeogenesis (*DoGMP*, *DoPMM*, *DoCSLA6*) in OE-DoMYB37 *D. officinale* protocorm-like bodies and control group. Significant differences between the Empty vector and OE-DoMYB37 seedlings grown under the same conditions (HP and LP) are indicated using asterisks (** $p < 0.01$; * $p < 0.05$; two-tailed Student's t-test)

DoCSLA6 expression was more higher in the DoSPX1 and DoMYB37 co-transformed group than MYB37 over-expressed alone (Fig. 5D). This suggests that DoSPX1 may work in concert with DoMYB37 to regulate the expression of *DoCSLA6*.

Discussion

Plants usually face LP environment, which limits their growth and development [20]. The protein-containing SPX domain is vital for the regulation of Pi signaling and Pi homeostasis, the SPX proteins sense phosphorus deficiency signaling and transduction the signal [21]. Duan's research shows that both AtSPX1 and AtSPX3 play

positive roles in plant adaptation to phosphate starvation, and AtSPX3 may have a negative feedback regulatory role in AtSPX1 response to phosphate starvation [22]. We found that DoSPX1 has a functional structural domain that reduces phosphate content in plants. *DoSPX1* can reduce phosphate accumulation in plants and promote the expression of *PSI* genes, thereby enhancing plant tolerance to LP environments.

MYB proteins play important roles in controlling metabolism regulation during the whole processes of plant growth and development. MYB TFs can be divided into four categories, namely, R1R2R3-MYB, R2R3-MYB, R1-MYB, and 4R-MYB [23]. R2R3-MYB S20 subfamily

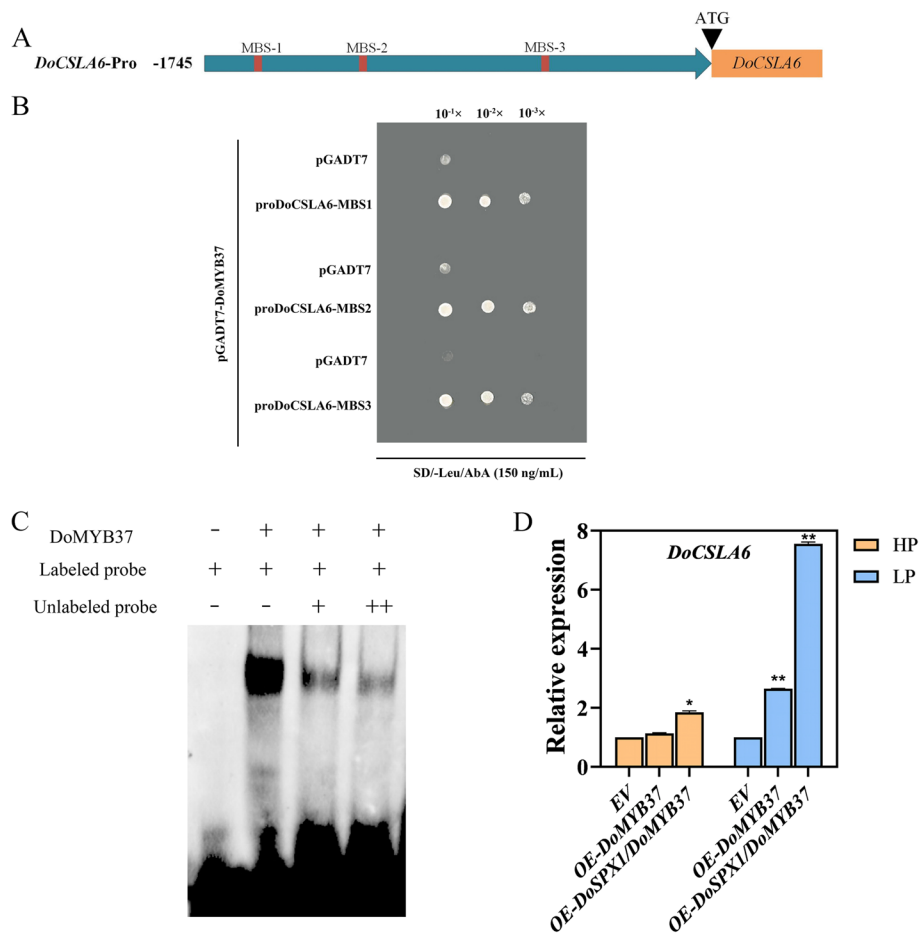


Fig. 5 Interaction between DoMYB37 and proDoCSLA6, and determination of DoCSLA6 expression and polysaccharide content in transgenic protocorm-like bodies and control group. **A** Validation of yeast monohybrid crosses. **B** Yeast one-hybrid between DoMYB37 and proDoCSLA6. **C** EMSA between DoMYB37 and proDoCSLA6. **D** The expression of DoCSLA6 in transgenic protocorm-like bodies. Significant differences between the Empty vector, OE-DoMYB37 and OE-DoMYB37/DoSPX1 seedlings grown under the same conditions (HP and LP) are indicated using asterisks (** $p < 0.01$; * $p < 0.05$; two-tailed Student's t-test)

(MYB-S20) transcription factors have been reported to be central regulators of plant responses to the LP pathway. MYB-S20 can sense the phosphorus signal transmitted by SPX [24, 25]. AtMYB62 is an R2R3-type MYB transcription factor. It connects Pi homeostasis and GA signaling during Pi starvation [26]. DoMYB37 had the highest homology with AtMYB62 and the expression of DoMYB37 was significantly increased in LP environment. DoMYB37 may involved in phosphorus signal in *D. officinale*.

In plants, SPX can interact with MYB, and then affects the transcriptional regulation of downstream phosphorus starvation-induced genes by MYB transcription factors. Previous studies indicated that rice SPX1 interacts with PHR2 (MYB-CC) in a Pi-dependent manner and acts as an inhibitor to repress PHR2 transcription

activation under Pi-replete conditions [27]. We verified that DoSPX1 can interact with DoMYB37 and affect the content of plant phosphates. By overexpressing DoMYB37 in tobacco and *D. officinale* protocorm-like bodies, we found that the expression of *PSI* genes was significantly up-regulated. However, whether the interaction of DoSPX1 with DoMYB37 affects the transcriptional regulation of these genes by DoMYB37 needs to be further explored.

The MYB family can response to stress signal like temperature, light and diseases, and then play transcriptional function in plant metabolic pathways by binding to the MBS sites of critical enzyme gene promoters [28, 29]. Metabolic pathways that MYB transcription factors can regulate include anthocyanins in *Arabidopsis thaliana* [30], Sugar in rice [31], salvanolic acid in *Salvia*

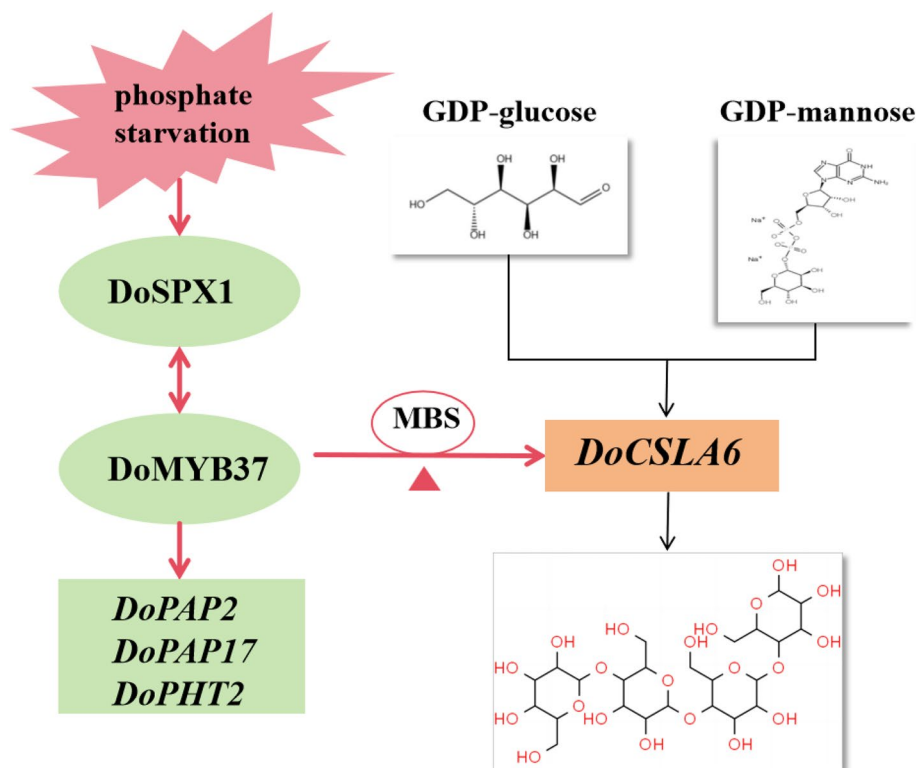


Fig. 6 *DoSPX1* and *DoMYB37* regulation of *DoCSLA6* expression in low phosphorus

multiorrhiza [28], paclitaxel biosynthesis in *Taxus chinensis* [32] and so on. Our previous study showed that *DoCSLA6* expression was elevated in LP. By yeast one hybridization and EMSA analysis, we found *DoCSLA6* is a target gene of *DoMYB37*. Expression of *DoCSLA6* was significantly increased in overexpressing *DoMYB37* *D. officinale* protocorm-like bodies. The expression level of the *DoCSLA6* gene in the co-transformation of *DoSPX1* and *DoMYB37* was much higher than that in the *DoMYB37* alone transformation. It suggests that *DoSPX1* and *DoMYB37* coregulated the expression of the *DoCSLA6* gene. However, whether the increase in the expression of *DoCSLA6* would affect the polysaccharides, mannose and glucose content of *D. officinale* needs to be further explored.

Conclusions

In *D. officinale*, both *DoSPX1* and *DoMYB37* respond to LP. Under LP environment, the early LP response factor *DoSPX1* was interact with *DoMYB37*, *DoMYB37* belong to S20 subfamily of MYB-R2R3 family. *DoMYB37* can bind the MBS site upstream of the *DoCSLA6* promoter and promote the expression of *DoCSLA6*. In the presence of *DoSPX1*, the promotion effect of *DoCSLA6* expression is more obvious. In summary, we established

the signal transduction model (“*DoSPX1-DoMYB37-DoCSLA6*”) of *D. officinale* in response to LP. The *DoCSLA6* can catalyzes the synthesis of glucomannan from GDP-glucose and GDP-mannose, we inferred that the increase of *DoCSLA6* expression may be the main reason for the increase of glucomannan, which needs to be further verified (Fig. 6).

Supplementary Information

The online version contains supplementary material available at <https://doi.org/10.1186/s12870-024-05512-8>.

Supplementary Material 1.

Supplementary Material 2: Supplementary Table 1. MS liquid medium formula. Supplementary Table 2. Name and sequence of the primers.

Supplementary Material 3: Supplementary Fig 1 Transformation of *D. officinale* protocorm-like bodies. Supplementary Fig 2. Subcellular localization of *DoSPX1*. Scale bars: 20µm. Supplementary Fig 3. Expression of *DoMYB37* at different phosphorus concentrations.

Acknowledgements

We thank Anhui Provincial Engineering Research Center for Development and Utilization of Local Characteristic Plant Resources for providing materials.

Authors' contributions

LL, JJ and ZY led the writing of the manuscript; YW, HX performed the experiment and collected the data; JR, HH and LL analysed and discussed the data; SX checked the grammar of the manuscript. All authors contributed critically to the drafts.

Funding

This work was supported by Natural Science Foundation of Hefei (2022036) and Nature Science Research Project of Anhui province (2108085MC80).

Availability of data and materials

The raw data generated in this study are available in Mendeley Data (<https://doi.org/10.17632/tddc3sww2k.1>). All data supporting the findings of this study are available from the corresponding authors upon request.

Declarations

Ethics approval and consent to participate

Not applicable.

Consent for publication

Not applicable.

Competing interests

The authors declare no competing interests.

Received: 19 June 2024 Accepted: 12 August 2024

Published online: 26 August 2024

References

- Chen W, Lu J, Zhang J, Wu J, Yu L, Qin L, Zhu B. Traditional Uses, Phytochemistry, Pharmacology, and Quality Control of *Dendrobium officinale* Kimura et. Migo. *Front Pharmacol.* 2021;12.
- Qu J, Tan S, Xie X, Wu W, Zhu H, Li H, Liao X, Wang J, Zhou Z-A, Huang S, Lu Q. *Dendrobium Officinale* Polysaccharide Attenuates Insulin Resistance and Abnormal Lipid Metabolism in Obese Mice. *Front Pharmacol.* 2021;12:659626.
- Wang L-X, Li C-Y, Hu C, Gong P-S, Zhao S-H. Purification and Structural Characterization of *Dendrobium officinale* Polysaccharides and Its Activities. *Chem Biodivers.* 2021;18:e2001023.
- Chen W-H, Wu J, Li X, Lu J, Wu W, Sun Y, Zhu B, Qin L. Isolation, structural properties, bioactivities of polysaccharides from *Dendrobium officinale* Kimura et. Migo: A review. *Int J Biol Macromol.* 2021;184:1000–13.
- Zhong C, Tian W, Chen H, Yang Y, Xu Y, Chen Y, Chen P, Zhu S, Li P, Du B. Structural characterization and immunoregulatory activity of polysaccharides from *Dendrobium officinale* leaves. *J Food Biochem.* 2022;46:e14023.
- Guo L, Qi J, Du D, Liu Y, Jiang X. Current advances of *Dendrobium officinale* polysaccharides in dermatology: a literature review. *Pharm Biol.* 2020;58:664–73.
- Hammond JP, Bennett MJ, Bowen HC, Broadley MR, Eastwood DC, May ST, Rahn C, Swarup R, Woolaway KE, White PJ. Changes in gene expression in *Arabidopsis* shoots during phosphate starvation and the potential for developing smart plants. *Plant Physiol.* 2003;132:578–96.
- Smith AP, Nagarajan VK, Raghothama KG. *Arabidopsis Pht1;5* plays an integral role in phosphate homeostasis. *Plant Signal Behav.* 2011;6:1676–8.
- Yang Z, Gao Z, Zhou H, He Y, Liu Y, Lai Y, Zheng J, Li X, Liao H. GmPTF1 modifies root architecture responses to phosphate starvation primarily through regulating *GmEXP2* expression in soybean. *Plant J.* 2021;107:525–43.
- Liu L, Xiang H, Shen H, Dong Y, Sun X, Cai Y, Fan H. Effects of low phosphorus stress on the main active ingredients and antioxidant activities of *Dendrobium officinale*. *Ind Crops Prod.* 2021;173:114095.
- He C, Wu K, Zhang J, Liu X, Zeng S, Yu Z, Zhang X, Teixeira da Silva JA, Deng R, Tan J, Luo J, Duan J. Cytochemical Localization of Polysaccharides in *Dendrobium officinale* and the Involvement of *DoCSLA6* in the Synthesis of Mannan Polysaccharides. *Front Plant Sci.* 2017;8:173.
- Liu N, Shang W, Li C, Jia L, Wang X, Xing G, Zheng W. Evolution of the SPX gene family in plants and its role in the response mechanism to phosphorus stress. *Open Biol.* 2018;8:170231.
- Ried MK, Wild R, Zhu J, Pipercevic J, Sturm K, Broger L, Harmel RK, Abriata LA, Hothorn LA, Fiedler D, Hiller S, Hothorn M. Inositol pyrophosphates promote the interaction of SPX domains with the coiled-coil motif of PHR transcription factors to regulate plant phosphate homeostasis. *Nat Commun.* 2021;12:384.
- Secco D, Wang C, Arpat BA, Wang Z, Poirier Y, Tyerman SD, Wu P, Shou H, Whelan J. The emerging importance of the SPX domain-containing proteins in phosphate homeostasis. *New Phytol.* 2012;193:842–51.
- Yang J, Zhao X, Chen Y, Li G, Li X, Xia M, Sun Z, Chen Y, Li Y, Yao L, Hou H. Identification, Structural, and Expression Analyses of SPX Genes in Giant Duckweed (*Spirodela polyrhiza*) Reveals Its Role in Response to Low Phosphorus and Nitrogen Stresses. *Cells.* 2022;11:1167.
- Zhang J, Zhou X, Xu Y, Yao M, Xie F, Gai J, Li Y, Yang S. Soybean SPX1 is an important component of the response to phosphate deficiency for phosphorus homeostasis. *Plant Sci.* 2016;248:82–91.
- He Y, Zhang X, Li L, Sun Z, Li J, Chen X, Hong G. SPX4 interacts with both PHR1 and PAP1 to regulate critical steps in phosphorus-status-dependent anthocyanin biosynthesis. *New Phytol.* 2021;230:205–17.
- Liu L, Xiang H, Song J, Shen H, Sun X, Tian L, Fan H. Genome-Wide Analysis of DoSPX Genes and the Function of *DoSPX4* in Low Phosphorus Response in *Dendrobium officinale*. *Front Plant Sci.* 2022;13:943788.
- Lescot M, Déhais P, Thijs G, Marchal K, Moreau Y, Van de Peer Y, Rouzé P, Rombauts S. PlantCARE, a database of plant cis-acting regulatory elements and a portal to tools for in silico analysis of promoter sequences. *Nucleic Acids Res.* 2002;30:325–7.
- Rouached H, Arpat AB, Poirier Y. Regulation of Phosphate Starvation Responses in Plants: Signaling Players and Cross-Talks. *Mol Plant.* 2010;3:288–99.
- Dong J, Ma G, Sui L, Wei M, Viswanathan S, Zhang R, Ge S, Li J, Zhang T, Christopher W, Henning J, Zhang H, An G, Chao D, Liu D, Lei M. Inositol Pyrophosphate InsP 8 Acts as an Intracellular Phosphate Signal in Arabidopsis. *Mol Plant.* 2019;11:1463–73.
- Duan K, Yi K, Dang L, Huang H, Wu W, Wu P. Characterization of a sub-family of Arabidopsis genes with the SPX domain reveals their diverse functions in plant tolerance to phosphorus starvation. *The Plant journal: for cell and molecular biology.* 2008;6:965–75.
- Dubos C, Stracke R, Grotewold E, Weisshaar B, Martin C, Lepiniec L. MYB transcription factors in *Arabidopsis*. *Trends Plant Sci.* 2010;15:573–81.
- Rubio V, Linhares F, Solano R, Martín AC, Iglesias J, Leyva A, Paz-Ares J. A conserved MYB transcription factor involved in phosphate starvation signaling both in vascular plants and in unicellular algae. *Genes Dev.* 2001;15:2122–33.
- Wykoff DD, Grossman AR, Weeks DP, Usuda H, Shimogawara K. Psr1, a nuclear localized protein that regulates phosphorus metabolism in Chlamydomonas. *Proc Natl Acad Sci U S A.* 1999;96:15336–41.
- Devaiah BN, Madhuvanathi R, Karthikeyan AS, Raghothama KG. Phosphate starvation responses and gibberellic acid biosynthesis are regulated by the MYB62 transcription factor in *Arabidopsis*. *Mol Plant.* 2009;2:43–58.
- Zhou J, Hu Q, Xiao X, Yao D, Ge S, Ye J, Li H, Cai R, Liu R, Meng F, Wang C, Zhu J-K, Lei M, Xing W. Mechanism of phosphate sensing and signaling revealed by rice SPX1-PHR2 complex structure. *Nat Commun.* 2021;12:7040.
- Yang R, Wang S, Zou H, Li L, Li Y, Wang D, Xu H, Cao X. R2R3-MYB Transcription Factor SmMYB52 Positively Regulates Biosynthesis of Salvanolic Acid B and Inhibits Root Growth in *Salvia miltiorrhiza*. *Int J Mol Sci.* 2021;22:9538.
- Zhang H, Liu Z, Luo R, Sun Y, Yang C, Li X, Gao A, Pu J. Genome-Wide Characterization, Identification and Expression Profile of MYB Transcription Factor Gene Family during Abiotic and Biotic Stresses in Mango (*Mangifera indica*). *Plants (Basel).* 2022;11:3141.
- Qin J, Zhao C, Wang S, Gao N, Wang X, Na X, Wang X, Bi Y. PIF4-PAP1 interaction affects MYB-bHLH-WD40 complex formation and anthocyanin accumulation in *Arabidopsis*. *J Plant Physiol.* 2022;268:153558.
- Chen Y-S, David Ho T-H, Liu L, Lee DH, Lee C-H, Chen Y-R, Lin S-Y, Lu C-A, Yu S-M. Sugar starvation-regulated MYB52 and 14-3-3 protein interactions enhance plant growth, stress tolerance, and grain weight in rice. *Proc Natl Acad Sci USA.* 2019;116:21925–35.
- Yu C, Luo X, Zhang C, Xu X, Huang J, Chen Y, Feng S, Zhan X, Zhang L, Yuan H, Zheng B, Wang H, Shen C. Tissue-specific study across the stem of *Taxus media* identifies a phloem-specific TmMYB3 involved in the transcriptional regulation of paclitaxel biosynthesis. *Plant J.* 2020;103:95–110.

Publisher's Note

Springer Nature remains neutral with regard to jurisdictional claims in published maps and institutional affiliations.